Catalytic Behaviors of the Heteropolytungstolanthanate (LnW10, Ln: Cerium, Neodymium, and Samarium) Anion on the Decomposition of Hydrogen Peroxide and Cyclohexanol Oxidation with H_2O_2 in a Homogeneous System

Ryuji SHIOZAKI, Hideya GOTO, and Yoshiya KERA*
Department of Applied Chemistry, Faculty of Science and Engineering, Kinki University, Higashiosaka, Osaka 577
(Received December 28, 1992)

In the presence of the heteropolytungstolanthanate anion (Ce(IV)$W_{10}O_{36}^{-8}$, Nd(III)$W_{10}O_{36}^{-9}$, and Sm(III)-$W_{10}O_{36}^{-9}$; LnW10) the kinetic behaviors of hydrogen peroxide decomposition and cyclohexanol oxidation with H_2O_2 were investigated. In CeW10 the H_2O_2 decomposition rate tended to reach almost a limited value with increasing H_2O_2 concentration, while in NdW10 and SmW10 it decreased considerably after reaching the maximum value in high H_2O_2. The kinetic behavior of LnW10 was reasonably explained by a reaction scheme in which an intermediate species is initially formed (IS_1) and then reacts further with H_2O_2 molecules to change the inactive species and, thus, to be removed from the catalytic cycle. Cyclohexanol was selectively oxidized with H_2O_2 to cyclohexanone according to the reaction order 0.6—0.8 on the H_2O_2 concentration until the high H_2O_2 region in the presence of all LnW10. The Arrhenius law concerning the overall rates of both reactions of H_2O_2 decomposition and cyclohexanol oxidation was maintained in any LnW10; further, a good compensation effect between the Arrhenius parameters, preexponential factor (log V_0) and apparent activation energy (E_{ap}), was found for both reactions in the series of LnW10. However, the empirical points concerning the log V_0 vs. E_{ap} plot in the oxidation alined in an inverse manner to those in H_2O_2 decomposition; that is, the order is CeW10<SmW10<NdW10 in the former and NdW10<SmW10<CeW10 in the latter. From this finding, both reactions were suggested to proceed via a common-intermediate species. Furthermore, it was elucidated that the more stable is the species, the more favorably are the alcohol molecules activated to the final products in the oxidation reaction.

The chemistry of heteropoly- and isopoly- oxometalates has been developed covering a wide scope.[1] Many investigators have been interested in the physicochemical properties of these oxometalates as catalysts. In fact, some of them have been used as catalysts for partial-oxidation and acid-base reaction processes;[2] the others as quite selective catalysts for the epoxidation of the olefins and carbonylation of alcohols with hydrogen peroxide and organic peroxides. Many mechanistic studies and confirmation of the intermediate species related to these reaction processes have also been attempted.[3—11]

Recently, we found an interesting catalytic property for a series of heteropolytungstolanthanate anions, (Ce(IV)$W_{10}O_{36}^{-8}$, Nd(III)$W_{10}O_{36}^{-9}$, and Sm(III)-$W_{10}O_{36}^{-9}$; abbreviated as LnW10 below) for the decomposition of H_2O_2 and a selective oxidation of alcohol with H_2O_2.[12] In CeW10, although the H_2O_2-decomposition rate tended to reach almost a limited value with increasing H_2O_2 concentration, in NdW10 and SmW10 it decreased considerably after reaching a maximum value at a high-H_2O_2 concentration. On the other hand, cyclohexanol oxidation with H_2O_2 was accelerated with increasing H_2O_2, even in such a high region, in the presence of any LnW10.

In the present study, the catalytic behaviors of LnW10 for both reactions were analyzed kinetically in detail. Through a discussion, the property of an intermediate species concerned with both reaction processes, perhaps a peroxo-complex, has been elucidated to differ considerably between the CeW10 and the NdW10, SmW10 catalyst systems. Such a peroxo-complex must play an important role in both the reaction processes as a common intermediate species.

Experimental

Preparation of Catalysts. LnW10 (Ln: Ce, Nd, and Sm) catalysts were prepared according to Peacock's procedure as follows.[13] $Na_2WO_4 \cdot 2H_2O$ (25 g, 75 mmol) was dissolved in 100 ml of ion-exchange water, the pH of which was adjusted to 7.2 by the addition of acetic acid. After heating at 90 °C with stirring, an aqueous solution containing $(NH_4)_4Ce(SO_4)_4 \cdot 2H_2O$ (4.75 g, 7.5 mmol) and a 1 equiv H_2SO_4 solution were added to make CeW10 form in the solution. The Nd and SmW10 solutions were prepared according to a similar procedure with CeW10, except for the use of $Nd(NO_3)_3$ and a nitric acid solution of Sm_2O_3 as the lanthanoid reagents. Those solutions were obtained after filtration and used as catalysts.

Instrumental Analyses. A guanidinium hydrochloride solution was added to the filtrate in order to obtain a precipitate of the guanidinium salt of LnW10. An X-ray fluorescence analysis was carried out using equipment provided by Rigaku Denki Co., Ltd. (Model 4455-M3) to determine the atomic ratio of tungsten to lanthanoid (W/Ln) in the guanidinium salts. The Rh-radiation (at 50 kV, and 50 mA) and LiF crystal as an analyzer were used. The FT-IR spectra of the guanidinium salts were also recorded on a Perkin-Elmer Model 1760X over the frequency range of 4000—450 cm^{-1} with a resolution of 4 cm^{-1} by the normal KBr-disk method, as an auxiliary measurement for the identification of LnW10 in the crystalline powder.

Apparatus and Procedures for Measuring the H_2O_2 Decomposition and Cyclohexanol Oxidation with H_2O_2. *t*-Butanol (15 ml) as a solvent and LnW10 solution (1.6 ml, 9.0×10^{-3}—6.4×10^{-2} mmol) as a catalyst

were mixed in a 200 ml Pyrex glass flask, to which a cooling condenser, a dropping funnel, and a joint connected to a vacuum pump were attached. The upper part of the cooling condenser was connected into a vacuum-line system equipped with a manometer. Before each reaction, the reaction vessel was allowed 5—10 min for thermal preequilibration. A given amount of an H_2O_2 solution (30%; 0.3—5.0 ml, 3.7—64 mmol) was then added into the catalyst system with stirring under a vacuum condition. The pressure in the reaction vessel (ca. 0.5 dm^3) was then adjusted to ca. 0.9 atm to initiate the reaction. The pressure change was measured manometrically during the initial stage of 10—40 min in order to evaluate the initial rate of H_2O_2 decomposition.

For the oxidation reaction of cyclohexanol with H_2O_2 *t*-butanol (15 ml), an LnW10 catalyst (1.6 ml, 4×10^{-2} mmol) solution and cyclohexanol (5.0 ml, 48.3 mmol) were mixed in the flask with stirring. While standing the mixture for 5—10 min, a given amount of an H_2O_2 solution (30%; 0.6—5.0 ml, 7.7—64 mmol) was added in order to initiate the reaction. A gas-chromatographic analysis was carried out using a Shimadzu Model GC-14A with a capillary column (Hicap-CBP-M25-025) and an FID detector to check the reaction during the initial stage of 0—90 min. The reaction temperatures were changed over the range of 30—65 °C with an accuracy of ±0.5 °C.

The reagents purchased from Kanto Chemical Co., Inc. were used without any treatment.

Results and Discussion

Identification of LnW10 Formed in an Aqueous Solution. The atomic ratio (W/Ln) in the guanidinium tungstolanthanates was determined by an X-ray fluorescence analysis to be approximately equal to 10. The FT-IR spectra of those compounds are illustrated in Fig. 1. The huge bands at 3500—3200 cm^{-1} and the sharp band at 1600 cm^{-1} are assignable to those of the guanidinium group. The characteristic bands for these compounds are summarized in Table 1. The crystal structure, which was determined by an X-ray analysis, indicates that isodecatungstate is formed by a coupling of pentatungstate; in the cerium-decatungstate anion (CeW10), the Ce(IV) ion is sandwiched by the pentatungstate units, that is, the Ce(IV) ion is inserted into the center of the decatungstate.[14] According to Sasaki et al.,[15,16] the ca. 940 cm^{-1} band is ascribable

Table 1. Characteristic Bands in Infrared Spectra of LnW10 Compounds

Sample[a]	Frequency/cm^{-1}		
	ν (Ln–O)	ν (W–Ot)	ν (W–Ob–W)
CeW10	Unknown	944	823, 760
NdW10	Unknown	926	847, 792
SmW10	Unknown	925	851, 804
$W_{10}O_{32}^{6-}$	—	960	900, 800

a) Guanidinium salts of LnW10 and tetrabutylammonium salts of $W_{10}O_{32}^{6-}$.[15,16]

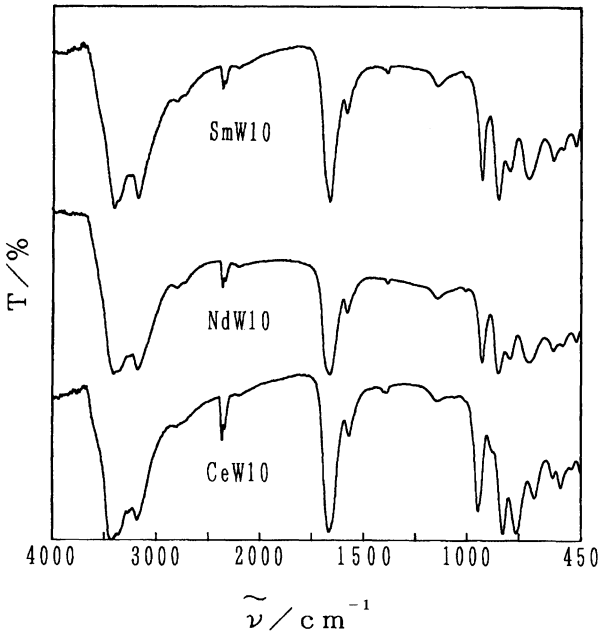

Fig. 1. FT-IR spectra of the prepared LnW10 guanidinium salts.

to the W=O stretching mode, and the ca. 850 and 790 cm^{-1} bands to the W–O–W stretching. Therefore, the formation of LnW10 in the solution was confirmed from measurements of the atomic ratio (W/Ln) and a comparison of the IR bands.

Kinetic Behaviors of H_2O_2 Decomposition in the Presence of LnW10. In the presence of CeW10, NdW10, and SmW10, the H_2O_2-decomposition rate was measured at 50 °C under various H_2O_2 concentrations, as shown in Fig. 2. The rate increased with the H_2O_2 concentration and reached a limited value above ca. 1.0 mol $dm^{-3}$of H_2O_2 addition in CeW10, while reaching a maximum value at ca. 1.0 mol dm^{-3}; it decreased considerably with a further addition in the NdW10 and SmW10 systems. With the CeW10 catalyst system, the temperature dependence of the rate was examined further, as shown in Fig. 3. The tendency for a decrease in the rate in the high-H_2O_2 region is also seen, even at lower temperatures, though the extent of this tendency is more or less small.

In the presence of CeW10, the reaction might be postulated to proceed by reaction schema (1) and (2), especially at lower H_2O_2 concentrations and temperatures. However, in the H_2O_2–NdW10 and SmW10 reacting systems, additional steps (3) and (4) could not be ignored, except for the lower H_2O_2 concentration:

$$H_2O_2 + (\mathrm{LnW10}) \underset{k_{-1}}{\overset{k_1}{\rightleftarrows}} IS_1, \quad (1)$$

$$IS_1 \xrightarrow{k_2} 1/2O_2 + H_2O + (\mathrm{LnW10}) \quad (2)$$

$$IS_1 + H_2O_2 \underset{k_{-3}}{\overset{k_3}{\rightleftarrows}} IS_2, \quad (3)$$

and

$$IS_2 + H_2O_2 \underset{k_{-4}}{\overset{k_4}{\rightleftarrows}} IS_3, \quad (4)$$

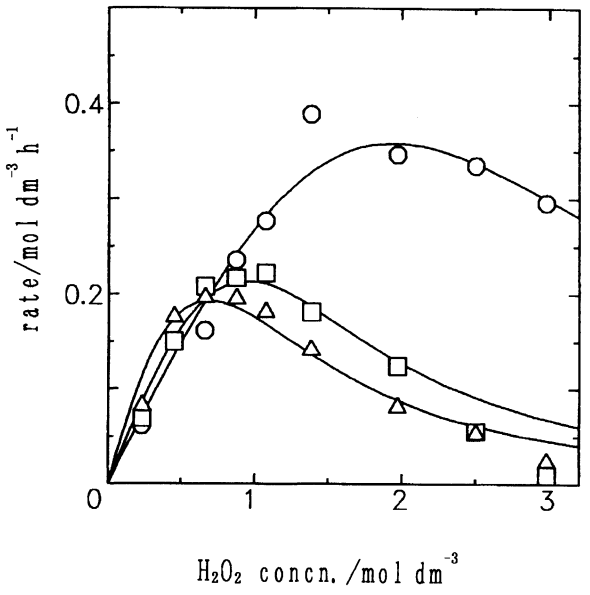

Fig. 2. H_2O_2-concentration dependence of the H_2O_2-decomposition rates in the presence of CeW10 (○), NdW10 (□), and SmW10 (△) at 50 °C. The full curves indicate the theoretical ones according to Eq. 6 in text. Catalyst: 1.6 ml, 4×10^{-2} mmol; H_2O_2: 0.3—5.0 ml, 3.7—64 mmol; *t*-BuOH: 15 ml.

Here, IS_1, IS_2, and IS_3 indicate some kind of intermediate species, and (LnW10) is not necessarily the LnW10 species, as it is in an aqueous solution. In fact, at a low-H_2O_2 concentration, such as 0.45 mol dm^{-3}, the decomposition rate at 40 °C depends upon ca. 1st-order kinetics for the catalyst concentration (Fig. 4), in which plots of the log(rate) versus log(catalyst-concentration) are given.

If steps (3) and (4) are ignored, the rate expression is deduced as

$$r = V_1[H_2O_2]/(K_1 + [H_2O_2]), \quad (5)$$

where $V_1 = k_2[LnW10]_0$, $K_1 = (k_{-1} + k_2)/k_1$ and $[LnW10]_0$ denotes the initial concentration of LnW10. In this case, it seemingly corresponds to the mechanism for enzyme kinetics, as formulated by Michaelis–Menten.[17] Such a kinetic behavior has been reported concerning H_2O_2 decomposition and hydrocarbon oxidation with H_2O_2 in the presence of many kinds of metal ions coordinated by various ligands.[4,5,18,19]

A general rate expression containing steps (3) and (4) is given as

$$r = V_1/((1 + (1/K_3)[H_2O_2] + (1/K_3K_4)[H_2O_2]^2 + K_1/[H_2O_2]), \quad (6)$$

where $K_3=(k_{-3}/k_3)$ and $K_4=(k_{-4}/k_4)$. In general, such an equation has been induced in the case of the presence

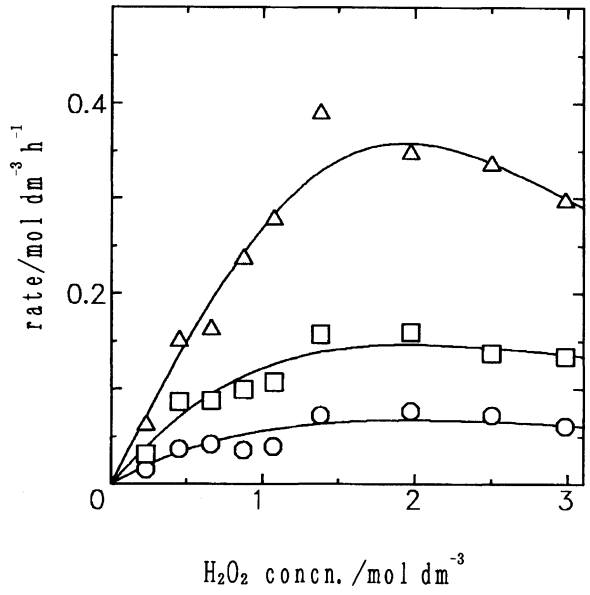

Fig. 3. Changes in the H_2O_2-decomposition rates with the H_2O_2 concentration on CeW10 at 30 °C (○), 40 °C (□), and 50 °C (△). Catalyst: 1.6 ml, 4×10^{-2} mmol; H_2O_2: 0.3—5.0 ml, 3.7—64 mmol; *t*-BuOH: 15 ml.

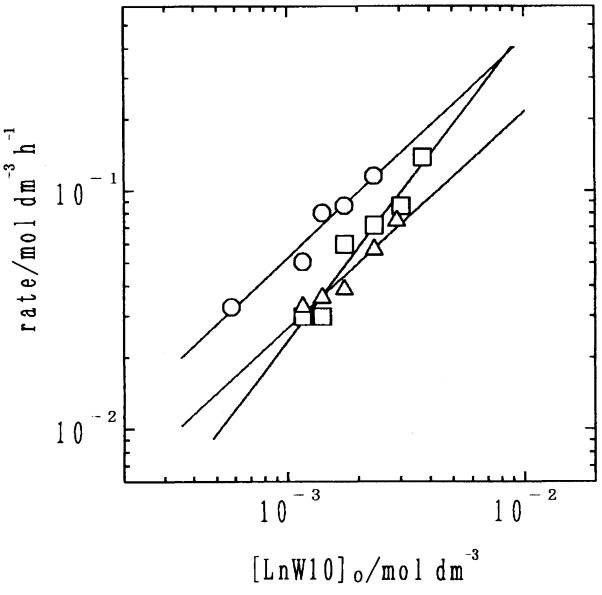

Fig. 4. Changes in the H_2O_2-decomposition rates with the concentration of CeW10 (○), NdW10 (□), and SmW10 (△) at 40 °C. Catalyst: 1.6 ml, 9.9—64×10^{-3} mmol; H_2O_2: 0.6 ml, 7.7 mmol; *t*-BuOH: 15 ml.

of an inhibitor instead of H_2O_2 molecules (substrate, itself).[20]

The inverse rate in Eq. 5 is expressed as

$$1/r = (K_1/V_1)(1/[H_2O_2]) + (1/V_1). \quad (7)$$

The relation of $1/r$ to $1/[H_2O_2]$ was examined with the data of the H_2O_2–CeW10 reacting system given in Fig. 3. The plots give linear lines to all the temperature runs, as shown in Fig. 5, although the points scatter more or less, especially at lower temperatures. We can easily estimate the V_1- and K_1-terms from the slope and the intersection on the vertical axes, respectively, as summarized in Table 2.

On the other hand, a set of the unknown parameters (K_3 and K_4 in Eq. 6) was determined so as to make the empirical points fit Eq. 6, especially in the higher H_2O_2 region. V_1 and K_1 in Table 2, which were determined based on the data in the lower H_2O_2 region, were used in a simulation procedure. The full curves that were added to the empirical points in Fig. 2 reveal the results of a simulation on Eq. 6. It has thus been clarified that the empirical data can be favorably explained by the assumed schema, Eqs. 1, 2, 3, and 4, as a possibility. If Eq. 2 is the rate-determining step, k_1 and $k_{-1} \gg k_2$ might hold, whether or not the contribution of such degradation steps as (3) and (4) so that K_1 can be regarded as being a stability constant for the intermediate species (IS_1) formed by step (1); that is,

$$K_1 = \exp(\Delta G_1/RT) = \exp(-(\Delta H_1 - T\Delta S_1)/RT), \quad (8)$$

and

$$\log(K_1) = -\Delta H_1/2.30RT + \Delta S_1/2.30R. \quad (9)$$

Since V_1 is equal to $k_2[\mathrm{LnW10}]_0$, the Arrhenius parameters for the elementary step (2) can be estimated from the temperature change given in Table 2. The temperature dependences of K_1 and k_2 according to Eqs. 9 and 11 are shown in Fig. 6.

$$K_1 = V_1 = k_2[\mathrm{LnW10}]_0 = A[\mathrm{LnW10}]_0 \exp(-E_a/RT) = A_0 \exp(-E_a/RT), \quad (10)$$

and

$$\log(V_1) = \log A_0 - E_a/RT. \quad (11)$$

From these linear relations we can estimate the physicochemical parameters, as summarized in Table 3.

At low H_2O_2 we measured the temperature dependences of the overall rate for the H_2O_2 decomposition. The Arrhenius plots are given in Fig. 7, and the parameters estimated from the linear plots are summarized in Table 4. In the case of CeW10, such degradation steps as (3) and (4) can be approximately ignored; at least at such a low H_2O_2, the parameters for

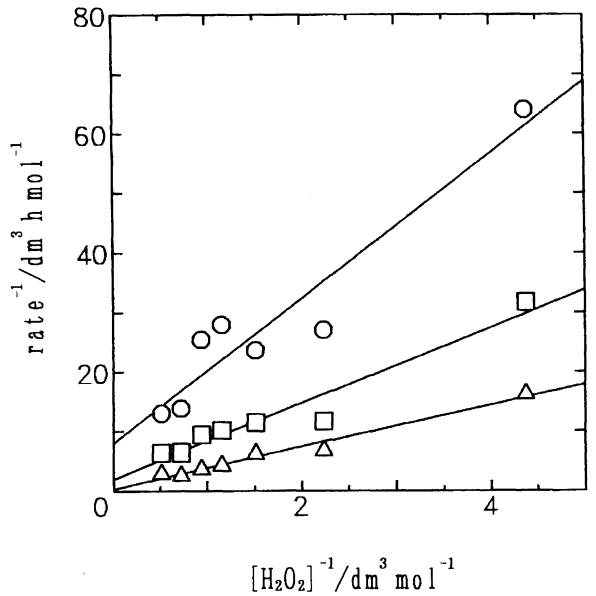

Fig. 5. Plots of $1/r$ versus $1/[H_2O_2]$ in Eq. 7; 30 °C (○), 40 °C (□), and 50 °C (△).

Table 2. Temperature Change of Kinetic Parameters, V_1 and K_1, in H_2O_2 Decomposition of CeW10

Temp	V_1	k_2 (turn over freq.)	K_1
K	mol dm^{-3} h^{-1}	h^{-1}	mol dm^{-3}
303	0.13	58.1	1.53
313	0.51	236	3.25
323	3.13	1456	11.0

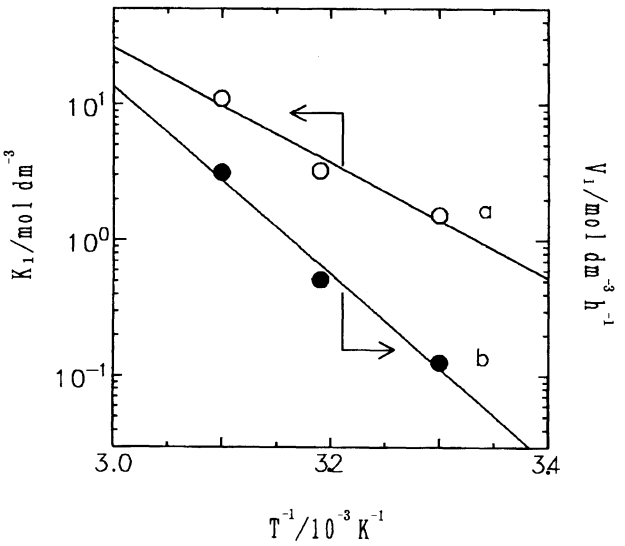

Fig. 6. Plots of the kinetic parameters for (a) K_1 (○) and (b) V_1 (●) versus $1/T$.

Table 3. Physicochemical Parameters for K_1 and V_1 in the H_2O_2 Reacting Process on CeW10

ΔH_1/kcal mol^{-1}	19
ΔS_1/cal mol^{-1} K^{-1}	65
E_a/kcal mol^{-1}	32
log A_0/mol dm^{-3} h^{-1}	22

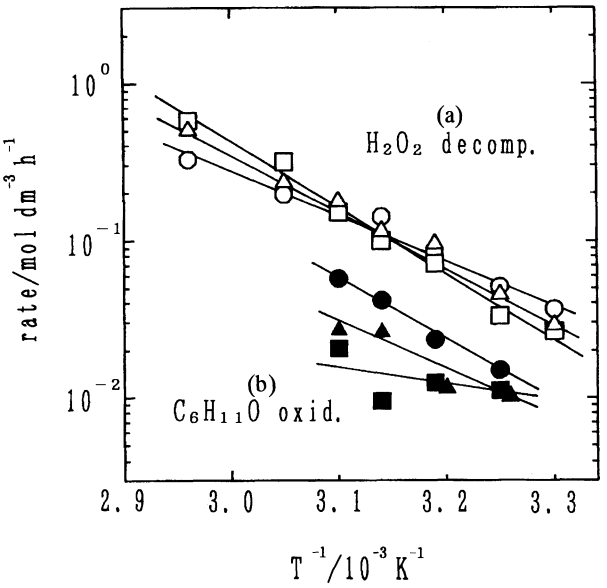

Fig. 7. Arrhenius plots for the overall rates of (a) H_2O_2 decomposition and (b) cyclohexanol oxidation for CeW10 (○) and (●), NdW10 (□) and (■), and SmW10 (△) and (▲). (a) Catalyst: 1.6 ml, 4×10^{-2} mmol; H_2O_2: 0.6 ml, 7.7 mmol; *t*-BuOH: 15 ml. (b) Catalyst: 1.6 ml, 4×10^{-2} mmol; H_2O_2: 5.0 ml, 64 mmol; Cyclohexanol: 5.0 ml, 48.3 mmol and *t*-BuOH: 15 ml.

Table 4. Arrhenius Parameters (E_{ap} and $\log V_0$) for Overall Rates of H_2O_2 Decomposition and $C_6H_{11}OH$ Oxidation with H_2O_2 in LnW10

LnW10	Reaction	E_{ap} / kcal mol^{-1}	$\log V_0$ / mol dm^{-3} h^{-1}
CeW10	H_2O_2 decomposition	13	7.9
	$C_6H_{11}OH$ oxidation	18	11
NdW10	H_2O_2 decomposition	19	12
	$C_6H_{11}OH$ oxidation	5.7	2.0
SmW10	H_2O_2 decomposition	16	10
	$C_6H_{11}OH$ oxidation	13	7.6

the elementary step (2) is certainly regarded as being quite correct. Therefore, by assuming that $k_{-1}\gg k_2$ and, thus, $K_1=k_{-1}/k_1$, the apparent activation energy (E_{ap}) should be comparable to the value of ($E_a-\Delta H_1$) in Table 3 ($E_{ap}=13$ kcal mol^{-1}). In fact, a good coincidence is seen in a comparison of both values. Thus, the energy diagram for the H_2O_2 decomposition process is reasonably described in Fig. 8.[20]

Furthermore, with the H_2O_2–NdW10 and SmW10 reacting systems, the contribution of Eqs. 3 and 4 should be weighted to a great extent; that is, the k_3- and k_4-terms should not be ignored. In these cases, based on parameters V_1 and K_1 estimated from the data at lower H_2O_2 concentrations, the empirical points in Fig. 2 were similarly simulated (as mentioned above). The full

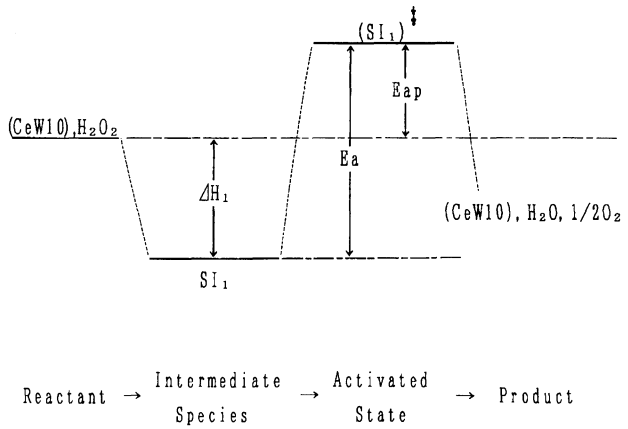

Fig. 8. Schematic energy diagram of the H_2O_2-decomposition process on CeW10.

curves added indicate the best fittings. In the Nd and SmW10 reacting systems, the contributions of the K_3- and K_4-terms relative to the V_1 and K_1-terms, in fact, were shown to be qualitatively quite larger than those in the CeW10 system. Thus, such a great decrease in the reaction rate with increasing H_2O_2 concentration in the NdW10 and SmW10 systems could be favorably understood by these discussions.

It has been reported by many authors that isopoly- and heteropoly-oxometalates of molybdenum and tungsten easily react with H_2O_2 to form various kinds of peroxo complexes.[6—12] In general, the initial structure of those oxometalates has been confirmed to be destroyed upon the formation of such peroxo-complexes by applying FT-IR, Raman, NMR techniques, and so on.[10,11]

We have attempted to detect such IS_1, IS_2, and IS_3-species based on a kinetic treatment by in-situ FT-Raman[21] and IR measurements. However, the structures of (LnW10) and IS_1 in Eq. 1 cannot be clarified. At present, it is also not clear whether or not species IS_1 and IS_2 can be converted reversively to IS_2 and IS_3 according to Eqs. 3 and 4, respectively.

Kinetic Behavior of Cycohexanol-Oxidation with H_2O_2 in the Presence of LnW10. In the presence of CeW10, NdW10, and SmW10, the initial rates of cyclohexanol-oxidation with H_2O_2 were measured at 40—60 °C under various H_2O_2-concentrations. Cyclohexanone was quite selectively obtained as the only product. The reaction rate increased with the H_2O_2-concentration in any LnW10 system, even though the H_2O_2-decomposition rate decreased considerably with NdW10 and SmW10 in the high-H_2O_2 region, as can be seen in Fig. 2. The log–log plots for the rate versus H_2O_2-concentration at 40 °C give roughly a linear relation to any catalyst system, as shown in Fig. 9. The reaction order on the H_2O_2 concentration was estimated to be nearly 0.7—0.8 from the slopes of the plots.

The temperature dependences of the rates on LnW10

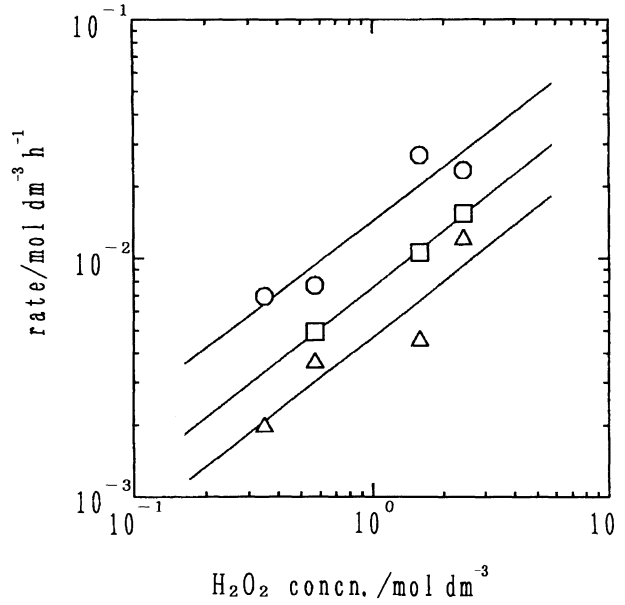

Fig. 9. Changes in the cyclohexanol-oxidation rates with the H_2O_2 concentration in the presences of CeW10 (○), NdW10 (□), and SmW10 (△) at 40 °C. Catalyst: 1.6 ml, 4×10^{-2} mmol; Cyclohexanol: 5.0 ml, 48.3 mmol; H_2O_2: 5.0 ml, 64 mmol; *t*-BuOH: 15 ml.

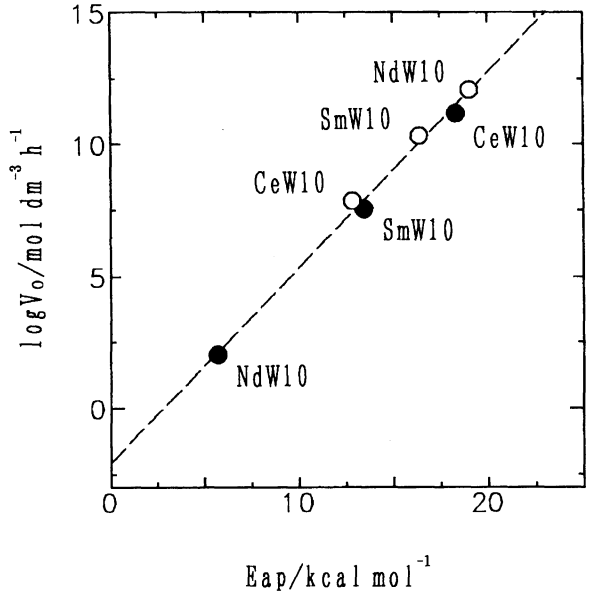

Fig. 10. Relationships between the Arrhenius parameters, apparent activation energy (E_{ap}) and prefactor (log V_0), for H_2O_2 decomposition (○) and cyclohexanol oxidation (●) in Table 4.

were measured; Arrhenius plots for the overall rates give a linear relationship to those catalyst systems, as added in Fig. 7. The Arrhenius parameters for the reaction has also been added to Table 4, in which the data for the oxidation are concerned with a high-H_2O_2 region (2.4 mol dm^{-3} H_2O_2), although those for the H_2O_2-decomposition with a low-H_2O_2 region (0.45 mol dm^{-3} H_2O_2). The relationship between the Arrhenius parameters for both reacting systems given in Table 4 was examined; the plots of the preexponential factor (log V_0) versus the apparent activation energy (E_{ap}) for the catalyst systems had a good linear relationship and, further, the data points for both reactions aligned almost along the same line, as shown in Fig. 10. Since a kinetic compensation effect was confirmed at the same time in those LnW10-catalyst systems, both reactions were suggested to occur through a similar intermediate state.[22] It should be noted that the points concerned with each catalyst align on the same straight line, but that the sequences are inverse to each other; that is, E_{ap} is higher in the order NdW10>SmW10>CeW10 for the H_2O_2 decomposition, and on the contrary, the order is CeW10>SmW10>NdW10 for the cyclohexanol oxidation.

These findings suggest that the intermediate species in the H_2O_2 decomposition, which might be some kind of peroxo-complex, also becomes a key species in the cyclohexanol oxidation. In the case that the intermediate species (IS_1) is more stable, the next decomposition step will be more restricted, so that a higher activation energy is required during H_2O_2 decomposition. That is, the order of the stability of the intermediate species is regarded as being IS_1(Nd–W)>IS_1(Sm–W)>IS_1(Ce–W). On the contrary, we can postulate that the more stable is the IS_1 species, and/or the stronger is the interaction between H_2O_2 and (LnW10), the cyclohexanol molecules are activated more favorably in the oxidation process. Thus, the sequence of E_{ap} for the oxidation becomes CeW10>SmW10>NdW10. This is an interpretation of the question why such an inverse alignment arose on plots of log V_0 versus E_{ap}.

Through the discussion, it is concluded that such a peroxo-complex plays an important rule in both reaction processes as a common intermediate species.

References

1) M. T. Pope, "Heteropoly and Isopoly Oxometalates," Springer, Berlin (1983).

2) M. Misono, K. Sakata, Y. Yoneda, and W. Ree, "Proc. 7th Intern. Congr. Catal.," Tokyo, 1980, Abstr., p. 1047, Kodansha (Tokyo)–Elsevier (Amsterdam), 1981; Y. Izumi and M. Otake, *Kagaku Sosetsu* (*in Japanese*), **34**, 116 (1982), and references therein.

3) R. A. Sheldon and J. K. Kochi, "Metal-Catalyzed Oxidations of Organic Compounds," Academic Press, New York (1981).

4) H. C. Stevens and A. J. Kaman, *J. Am. Chem. Soc.*, **87**, 734 (1965).

5) E. S. Gould, R. R. Hiatt, and K. C. Irwin, *J. Am. Chem. Soc.*, **90**, 4573 (1968); C. Su, J. W. Reed, and E. Gould, *Inorg. Chem.*, **12**, 337 (1973).

6) S. E. Jacobson, R. Tang, and F. Mares, *Inorg. Chem.*, **17**, 3055 (1978); S. E. Jacobson, D. A. Muccigrosso, and F. Mares, *J. Org. Chem.*, **44**, 921 (1979).

7) Y. Ishii, K. Yamawaki, T. Yoshida, T. Ura, and M. Ogawa, *J. Org. Chem.*, **52**, 1868 (1987); K. Yamawaki, Y. Ishii, and M. Ogawa, *Chem. Express*, **1**, 95 (1986).
8) C. Venturello and M. Ricci, *J. Org. Chem.*, **51**, 1599 (1986).
9) K. Kaneda, Y. Kawanishi, K. Jitsukawa, and S. Teranishi, *Tetrahedron Lett.*, **24**, 5009 (1983).
10) N. J. Campball, A. C. Dengel, C. J. Edwards, and W. P. Griffith, *J. Chem. Soc., Dalton Trans.*, **1989**, 1203, and reference therein.
11) C. Aubry, G. Ghottard, N. Platzer, J. M. Bregeault, R. Thouvenot, F. Chauveau, C. Huet, and H. Ledon, *Inorg. Chem.*, **30**, 4409 (1991).
12) H. Goto, R. Shiozaki, and Y. Kera, "68th Ann. Meet. Catal. Soc. Japan," Sapporo, 1991, Abstr., 3H312; R. Shiozaki and Y. Kera, *Shokubai*, **34**, 114 (1992).
13) R. D. Peacock and T. J. R. Weakley, *J. Chem. Soc. A*, **1971**, 1836.
14) J. Iball, J. N. Low, and T. J. R. Weakley, *J. Chem. Soc., Dalton Trans.*, **1974**, 2021.
15) Y. Sasaki and N. Miyazawa, *J. Fac. Sci. Technol. Kinki Univ.*, **26**, 217 (1990).
16) T. Yamase, Y. Sasaki, and T. Motowaki, *Inorg. Chim. Acta*, **121**, L19 (1986); T. Yamase, M. Matsuzawa, and Y. Sasaki, *Inorg. Chim. Acta*, **127**, L9 (1987).
17) W. J. Moore, "Physical Chemistry," 3rd ed, Prentice Hall, Inc., NJ (1962), p. 312.
18) J. H. Wang, *J. Am. Chem. Soc.*, **77**, 4715 (1955).
19) C. M. Diken, F. L. Lu, M. W. Nee, and T. C. Bruice, *J. Am. Chem. Soc.*, **107**, 5776 (1985).
20) T. Keii, "Shokubai Kagaku (Catalyst Chemistry)," Kagaku-Doujin, Tokyo (1981), pp. 86 and 170.
21) R. Shiozaki, M. Morimoto, E. Nishio, and Y. Kera, *Chem. Express*, **8**, 361 (1993).
22) Y. Kera and M. Negoro, *J. Catal.*, **99**, 198 (1986), and references Cited therein.